

# High field magnetotransport in composite conductors: The effective medium approximation revisited

David J. Bergman<sup>a,b</sup> and David G. Stroud<sup>b</sup>

<sup>a</sup>*School of Physics and Astronomy, Raymond and Beverly Sackler Faculty of Exact Sciences  
Tel Aviv University, Tel Aviv 69978, Israel*

<sup>b</sup>*Department of Physics, The Ohio State University, Columbus, OH 43210-1106  
(February 1, 2008)*

The self consistent effective medium approximation (SEMA) is used to study three-dimensional random conducting composites under the influence of a strong magnetic field  $\mathbf{B}$ , in the case where all constituents exhibit isotropic response. Asymptotic analysis is used to obtain almost closed form results for the strong field magnetoresistance and Hall resistance in various types of two- and three-constituent isotropic mixtures for the entire range of compositions. Numerical solutions of the SEMA equations are also obtained, in some cases, and compared with those results. In two-constituent free-electron-metal/perfect-insulator mixtures, the magnetoresistance is asymptotically proportional to  $|\mathbf{B}|$  at *all concentrations above the percolation threshold*. In three-constituent metal/insulator/superconductor mixtures a line of critical points is found, where the strong field magnetoresistance switches abruptly from saturating to non-saturating dependence on  $|\mathbf{B}|$ , at a certain value of the insulator-to-superconductor concentration ratio. This transition appears to be related to the phenomenon of anisotropic percolation.

To appear in Phys. Rev. B

## I. INTRODUCTION

Over the years, the Bruggeman self consistent effective medium approximation (SEMA) for the bulk effective electrical conductivity of a composite medium<sup>1,2</sup> has spawned a number of extensions and generalizations. Those include a SEMA for elastic stiffness of a composite medium,<sup>3,4</sup> a SEMA for a weakly nonlinear conducting composite,<sup>5</sup> and a SEMA for a strongly nonlinear (power law) conducting composite.<sup>6,7</sup> They also include a SEMA for a linear conducting composite medium where the constituents are characterized by *nonscalar conductivity tensors*.<sup>8,9</sup> Such approximations are needed to study the nonscalar conductivity due to an externally applied magnetic field  $\mathbf{B}$ .<sup>8-12</sup>

In composite conductors, the microstructure can induce a dependence of the Ohmic resistivity on magnetic field (i.e., magnetoresistance) even when none of the constituents exhibits any such dependence by itself. This arises because the local current density  $\mathbf{J}(\mathbf{r})$  acquires spatial fluctuations in both magnitude and direction, as a result of the heterogeneity or microstructure. Those are reflected in similar fluctuations of the local Hall (electric) field  $\mathbf{E}_H(\mathbf{r})$ , which usually has a nonzero component along the direction of the volume averaged current density  $\langle \mathbf{J} \rangle$ . The volume average of that component of  $\mathbf{E}_H$  vanishes to leading order in  $\mathbf{B}$ , but in higher orders that average is usually nonzero. As a result, the bulk effective Ohmic resistivity of the composite usually depends upon  $\mathbf{B}$ . The SEMA developed in Refs. 8,9 was used in numerical studies of magnetotransport in various types of composites, where this induced magnetoresistance played an important role.<sup>9,11,13,14</sup> It was also used in an unpublished discussion of asymptotic strong field behavior of magnetoresistance in a free-electron-conductor host with open orbit inclusions.<sup>15</sup>

More recently, it was shown that this type of SEMA, when applied to composites with a *columnar microstructure*, often violates some exact relations which exist between the different components of the bulk effective resistivity tensor. A modified SEMA has been developed which incorporates those exact relations [the “columnar unambiguous self-consistent effective medium approximation (CUSEMA)”]; it has been used for a detailed asymptotic analysis of metal/insulator ( $M/I$ ) and metal/superconductor ( $M/S$ ) random columnar mixtures in the strong field limit.<sup>16</sup> Very recently, the CUSEMA was applied to a three-constituent metal/insulator/superconductor ( $M/I/S$ ) random columnar composite mixture; a line of critical points was found to appear whenever the  $I$  and the  $S$  constituents are present in equal amounts, i.e., when their volume fractions  $p_I$  and  $p_S$  are equal. At this point, the asymptotic strong field behavior of the magnetoresistance switches abruptly from saturated for  $p_S > p_I$  to nonsaturating  $\propto |\mathbf{B}|^2$  behavior for  $p_S < p_I$ .<sup>17</sup> This critical point exhibits scaling behavior, along with critical exponents and scaling functions, all of which were determined, approximately, using CUSEMA.

In this article we present a theoretical study of magnetoresistance in three-dimensional disordered composite media. Some of the systems we study are isotropic, two-constituent mixtures of isotropic constituents. In this category, we consider mixtures of normal conductors ( $M_1/M_2$ ),  $M/I$  mixtures, and  $M/S$  mixtures. No “intrinsic anisotropy” is allowed for any constituent; thus, open orbit constituents are not considered. The normal conducting constituents

can be simple free-electron conductors, in which case only the Hall resistivity depends upon  $\mathbf{B}$ , or they can be more complicated conductors or semiconductors where the Ohmic resistivity also depends upon  $\mathbf{B}$ . But the longitudinal Ohmic resistivity  $\rho_{\parallel}$  (along  $\mathbf{B}$ ) and the transverse Ohmic resistivity  $\rho_{\perp}$  (perpendicular to  $\mathbf{B}$ ), as well as the Hall resistivity  $\rho_{\text{Hall}}$ , are assumed to be *independent of the direction* of  $\mathbf{B}$ . We also consider an  $M/I/S$  mixture, again with isotropic constituents, an isotropic microstructure, and  $\rho_{\parallel}^{(M)}$ ,  $\rho_{\perp}^{(M)}$ ,  $\rho_{\text{Hall}}^{(M)}$  of the  $M$  constituent which are independent of the direction of  $\mathbf{B}$ .

The SEMA equations for these composites do not admit exact closed form solutions. However, in the strong field limit, asymptotic analysis can be applied to those equations. The strong field limit means that  $|H| \gg 1$ , where  $H$  is the Hall-to-transverse-Ohmic resistivity ratio in a metallic or normal conducting constituent

$$H \equiv \frac{\rho_{\text{Hall}}^{(M)}}{\rho_{\perp}^{(M)}} = \mu |\mathbf{B}|, \quad (1.1)$$

and where  $\mu$  is the Hall mobility; note that  $\mu$  and  $\rho_{\text{Hall}}^{(M)}$ , and therefore also  $H$ , can be either positive or negative, depending on the sign of the majority charge carriers. This asymptotic analysis often leads to results in simple closed form, or at least “almost closed form.” In several cases we have also solved the SEMA equations numerically in order to compare with the asymptotic analysis.

The rest of this article is organized as follows. In Section II we briefly review the SEMA, using a formulation that reproduces the usual SEMA equations for non-scalar conducting constituents in terms of depolarization coefficients of the different types of inclusions. In Sections III and IV asymptotic analysis is used to find almost closed form solutions to those equations for a number of special cases. Those asymptotic solutions are compared, in some cases, with numerical solutions of the same equations. In Section III, we treat the special case of an  $M_1/M_2$  binary mixture. All concentrations are considered, starting from the limit of extreme dilution and all the way to the percolation threshold. In Section IV,  $M/I/S$  three-constituent mixtures are treated using asymptotic analysis. A line of critical points is found where the strong field response changes abruptly in the manner of a second-order-phase-transition, as the relative amounts of  $I$  and  $S$  are varied. Critical exponents, a scaling variable, and scaling functions are found which characterize the critical behavior. We also discuss  $M/S$  and  $M/I$  mixtures as special cases of these three-constituent composites. A linear dependence of the magnetoresistance upon  $|\mathbf{B}|$  is found in free-electron-metal/perfect-insulator mixtures for *all concentrations* where the mixture conducts macroscopically.

Section V provides a discussion of the results. We formulate a physical picture of the microscopic processes (i.e., local current flow patterns) which lead to some of the results found in previous sections for the macroscopic response. We also discuss a possible relation between the line of critical points found in the macroscopic magnetotransport of three-constituent  $M/I/S$  mixtures and the phenomenon of anisotropic percolation.

## II. REVIEW OF SEMA FOR THE CURRENT PROBLEMS

The self consistent effective medium approximation (SEMA) for constituents with arbitrary conductivity tensors, which appear in the system as ellipsoidal grains, was developed many years ago by one of the present authors<sup>9</sup>. This development followed more specialized versions, such as all scalar conductivities,<sup>1,2</sup> and later, strong field magnetotransport<sup>8</sup> and weak field Hall conductivity.<sup>10</sup> Here we describe a slightly different formulation of the general theory of Ref. 9. We use this formulation to find asymptotic physical solutions of the SEMA equations when the magnetic field is very strong. This formulation was described in detail in Ref. 16. A similar formulation also appeared in Ref. 12.

In practice, the SEMA requires that one calculate the electric field  $\mathbf{E}_1$  induced inside a single inclusion, with conductivity tensor  $\hat{\sigma}_{\text{inc}}$ , embedded in an otherwise uniform host with conductivity tensor  $\hat{\sigma}_{\text{host}}$ , when an external uniform electric field  $\mathbf{E}_0$  is applied at large distances. Whenever the inclusion is an ellipsoid,  $\mathbf{E}_1$  is *uniform*, whatever the values of  $\hat{\sigma}_{\text{inc}}$ ,  $\hat{\sigma}_{\text{host}}$ . Obviously,  $\mathbf{E}_1$  will be a homogeneous linear function of  $\mathbf{E}_0$ , which can be written with the help of a matrix  $\hat{\gamma}_{\text{inc}}(\hat{\sigma}_{\text{inc}}, \hat{\sigma}_{\text{host}})$

$$\mathbf{E}_1 = \hat{\gamma}_{\text{inc}} \cdot \mathbf{E}_0. \quad (2.1)$$

If the coordinate axes are taken to lie along the principal axes of the symmetric part of the tensor  $\hat{\sigma}_{\text{host}}$ , then we can write

$$\left( \frac{1}{\hat{\gamma}_{\text{inc}}} \right)_{\alpha\gamma} = \delta_{\alpha\gamma} - \sum_{\beta} \frac{n_{\alpha\beta} \delta\sigma_{\beta\gamma}}{\left( \sigma_{\alpha\alpha}^{(\text{host})} \sigma_{\beta\beta}^{(\text{host})} \right)^{1/2}}, \quad (2.2)$$

$$\delta\hat{\sigma} \equiv \hat{\sigma}_{\text{host}} - \hat{\sigma}_{\text{inc}}. \quad (2.3)$$

The factors  $n_{\alpha\beta}$  are elements of the depolarization tensor  $\hat{n}$ , *not of the actual physical inclusion*, but of its image after the coordinate axes have been rescaled by the following transformation

$$x' \equiv \frac{x}{\sqrt{\sigma_{xx}^{(\text{host})}}}, \quad y' \equiv \frac{y}{\sqrt{\sigma_{yy}^{(\text{host})}}}, \quad z' \equiv \frac{z}{\sqrt{\sigma_{zz}^{(\text{host})}}}. \quad (2.4)$$

Under this transformation, the ellipsoidal inclusion is usually transformed into another ellipsoidal shape, with major axes that have different lengths and different orientations compared to those of the physical inclusion. The SEMA is then obtained by setting  $\hat{\sigma}_{\text{host}} = \hat{\sigma}_e$ , and demanding that the small but exactly calculable change in  $\langle \mathbf{J} \rangle$ , caused by one isolated ellipsoidal inclusion, vanish when averaged over the different kinds of inclusions. This leads to the following self consistency equations for the elements of  $\hat{\sigma}_e$

$$0 = \langle (\hat{\sigma}_e - \hat{\sigma}_{\text{inc}}) \cdot \hat{\gamma}_{\text{inc}}(\hat{\sigma}_{\text{inc}}, \hat{\sigma}_e) \rangle. \quad (2.5)$$

In general, these are nonlinear equations, in which there appear *non-elementary transcendental functions* of the elements of  $\hat{\sigma}_e$ . Thus, closed form solutions are usually out of the question. However, we will show below that asymptotic solutions, for a very strong magnetic field  $\mathbf{B}$ , can sometimes be obtained in almost closed form. For smaller values of  $\mathbf{B}$ , the SEMA equations can be solved numerically, where needed; these solutions are discussed below.

We assume the following forms for the resistivity matrices of the host and inclusion:

$$\hat{\rho}_{\text{host}} = \rho_0 \begin{pmatrix} \alpha & -\beta & 0 \\ \beta & \alpha & 0 \\ 0 & 0 & \lambda \end{pmatrix}, \quad \hat{\rho}_{\text{inc}} = \rho_1 \begin{pmatrix} 1 & -H & 0 \\ H & 1 & 0 \\ 0 & 0 & \nu \end{pmatrix}. \quad (2.6)$$

These forms mean that both the host and the inclusion have isotropic electrical response, and that the only physically selected direction is that of the magnetic field  $\mathbf{B}$ , which is always taken to lie along  $z$ . This implies that the microstructure, as well as the electrical response of all the constituents, are isotropic. The  $\alpha$  coefficient in  $\hat{\rho}_{\text{host}}$  is actually redundant. We will sometimes exploit that redundancy by choosing  $\rho_0$  of the bulk effective resistivity tensor of the composite medium to be the same as one of the constituent values of  $\rho_1$ . The conductivity tensors  $\hat{\sigma}_{\text{host}}$ ,  $\hat{\sigma}_{\text{inc}}$  are easily found by inverting  $\hat{\rho}_{\text{host}}$ ,  $\hat{\rho}_{\text{inc}}$ .

Because we are considering isotropic microstructures, we will assume that all the constituents appear as spherical inclusions in the fictitious uniform effective medium host. In that case we find

$$\hat{\gamma}_{\text{inc}}(\hat{\sigma}_{\text{inc}}, \hat{\sigma}_{\text{host}}) = \begin{pmatrix} \frac{1}{D_{\text{inc}}} \left( 1 - n_x + n_x \frac{\rho_0}{\rho_1} \frac{\alpha^2 + \beta^2}{\alpha(1+H^2)} \right) & \frac{n_x}{D_{\text{inc}}} \left( \frac{\beta}{\alpha} - \frac{\rho_0}{\rho_1} \frac{\alpha^2 + \beta^2}{\alpha} \frac{H}{1+H^2} \right) & 0 \\ -\frac{n_x}{D_{\text{inc}}} \left( \frac{\beta}{\alpha} - \frac{\rho_0}{\rho_1} \frac{\alpha^2 + \beta^2}{\alpha} \frac{H}{1+H^2} \right) & \frac{1}{D_{\text{inc}}} \left( 1 - n_x + n_x \frac{\rho_0}{\rho_1} \frac{\alpha^2 + \beta^2}{\alpha(1+H^2)} \right) & 0 \\ 0 & 0 & \frac{1}{1 - n_z + n_z \lambda / \nu} \end{pmatrix}, \quad (2.7)$$

where

$$D_{\text{inc}} \equiv \left( 1 - n_x + n_x \frac{\rho_0}{\rho_1} \frac{\alpha^2 + \beta^2}{\alpha(1+H^2)} \right)^2 + n_x^2 \left( \frac{\beta}{\alpha} - \frac{\rho_0}{\rho_1} \frac{\alpha^2 + \beta^2}{\alpha} \frac{H}{1+H^2} \right)^2, \quad (2.8)$$

and where  $n_x, n_y = n_x$ , and  $n_z$  are the depolarization factors of the spheroidal shape into which the spherical inclusion was transformed by Eqs. (2.4). Those depolarization factors are elementary transcendental functions of  $\alpha, \beta, \lambda$ .<sup>18</sup> Thus, the elements of  $\hat{\gamma}_{\text{inc}}$  are also non-algebraic functions of those parameters. Consequently, the equations obtained for those parameters, by applying the self consistency requirements implied by Eq. (2.5), will usually be complicated, coupled, non-algebraic equations which lack closed form solutions in terms of elementary functions. This makes the qualitative study of their physical solutions highly nontrivial.

### III. APPLICATION OF SEMA TO MAGNETORESISTANCE OF AN $M_1/M_2$ MIXTURE

As an illustration, we now work out the effective resistivity tensor for a binary composite of two normal metals, using the SEMA. Two other special cases—a composite of normal metal and insulator, and one of normal metal and perfect conductor—will be discussed in the next section as special cases of three-constituent mixtures.

In the present case, the bulk effective resistivity tensors of the two constituents are assumed to have the similar forms

$$\hat{\rho}_1 = \rho_1 \begin{pmatrix} 1 & -H_1 & 0 \\ H_1 & 1 & 0 \\ 0 & 0 & \nu_1 \end{pmatrix}, \quad \hat{\rho}_2 = \rho_2 \begin{pmatrix} 1 & -H_2 & 0 \\ H_2 & 1 & 0 \\ 0 & 0 & \nu_2 \end{pmatrix}, \quad (3.1)$$

while the bulk effective resistivity tensor is assumed to have the form

$$\hat{\rho}_e = \rho_1 \begin{pmatrix} \alpha & -\beta & 0 \\ \beta & \alpha & 0 \\ 0 & 0 & \lambda \end{pmatrix}. \quad (3.2)$$

Note that  $\hat{\rho}_e$  and  $\hat{\rho}_1$  have been expressed in terms of the same resistivity factor  $\rho_1$ . The forms (3.1) and (3.2) imply that both constituents are isotropic conductors, as is the composite, and that the magnetic field  $\mathbf{B}$  is applied along  $z$ . They include the case where both  $\hat{\rho}_1$  and  $\hat{\rho}_2$  represent simple free-electron or free-hole conductors. They also include more general types of conductors, where the Ohmic resistivities and Hall mobility depend upon  $|\mathbf{B}|$ .

Application of Eq. (2.5) leads to three coupled equations for the unknown parameters  $\alpha$ ,  $\beta$ ,  $\lambda$ , which arise from the  $zz$ ,  $xy$ , and  $xx$  components of that tensorial equation [the  $xx$  and  $yy$  components lead to the same equation, as do the  $xy$  and  $yx$  components, while the  $xz$ ,  $zx$ ,  $yz$ , and  $zy$  components of Eq. (2.5) vanish identically;  $p_1$  and  $p_2 = 1 - p_1$  denote the volume fractions of the two constituents]:

$$0 = \frac{1 - n_z}{\lambda} - \frac{\rho_1}{\rho_2} \frac{\lambda n_z}{\nu_1 \nu_2} + n_z \left( \frac{p_2}{\nu_1} + \frac{p_1}{\nu_2} \frac{\rho_1}{\rho_2} \right) - (1 - n_z) \left( \frac{p_2}{\nu_2} \frac{\rho_1}{\rho_2} + \frac{p_1}{\nu_1} \right), \quad (3.3)$$

$$0 = \left( p_2 \frac{D_1}{D_2} + p_1 \right) \frac{\beta}{\alpha^2 + \beta^2} - p_2 \frac{D_1}{D_2} \frac{\rho_1}{\rho_2} \frac{H_2}{1 + H_2^2} - p_1 \frac{H_1}{1 + H_1^2}, \quad (3.4)$$

$$0 = \left( p_2 \frac{D_1}{D_2} + p_1 \right) \left( \frac{\alpha}{\alpha^2 + \beta^2} - \frac{n_x}{\alpha} \right) + \frac{p_2}{1 + H_2^2} \frac{D_1}{D_2} \frac{\rho_1}{\rho_2} \left[ n_x \left( 2 + \frac{2\beta H_2}{\alpha} - \frac{\rho_1}{\rho_2} \frac{\alpha^2 + \beta^2}{\alpha} \right) - 1 \right] + \frac{p_1}{1 + H_1^2} \left[ n_x \left( 2 + \frac{2\beta H_1}{\alpha} - \frac{\alpha^2 + \beta^2}{\alpha} \right) - 1 \right]. \quad (3.5)$$

Not surprisingly, these equations do not admit any closed form solutions. Since we are interested in the behavior of  $\alpha$ ,  $\beta$ ,  $\lambda$  at strong fields, we will apply asymptotic analysis for the limiting case where  $H_1 \equiv H$  and  $H_2 \equiv \omega H$  are both much greater than 1, i.e.,  $\omega$  remains bounded but  $|H| \gg 1$ . All other physical parameters of the two constituents are also assumed to remain bounded. From Eq. (3.3) it follows that  $\lambda$  must also remain bounded. We have tried various ansatzes for the asymptotic behavior of  $\alpha$ ,  $\beta$ , and proceeded to examine whether they lead to a mathematically consistent and physically admissible solution. The only ansatz that could satisfy those requirements was

$$\beta \cong \beta_0 H, \quad \alpha \cong \alpha_0 |H|^{2/3}, \quad \lambda \cong \lambda_0, \quad (3.6)$$

where  $\alpha_0$ ,  $\beta_0$ ,  $\lambda_0$  are positive dimensionless coefficients. It follows from this ansatz that the transformation of Eqs. (2.4) changes the spherical inclusions into flat, pancake shaped or oblate spheroids, with the short major axis along  $z$ , and with eccentricity  $e$  that diverges as  $|H| \rightarrow \infty$ . The eccentricity  $e$  and depolarization factors are given by<sup>18</sup>

$$e = \left( \frac{\alpha^2 + \beta^2}{\alpha \lambda} - 1 \right)^{1/2} \cong \frac{\beta_0}{\sqrt{\alpha_0 \lambda_0}} |H|^{2/3} \gg 1, \quad (3.7)$$

$$n_z = \frac{1 + e^2}{e^3} (e - \arctan e) \cong 1 - \frac{\pi}{2e} \quad (3.8)$$

$$\cong 1 - \frac{\pi}{2} \frac{\sqrt{\alpha_0 \lambda_0}}{\beta_0} |H|^{-2/3} \cong 1, \quad (3.9)$$

$$n_x = n_y = \frac{1}{2} (1 - n_z) = \frac{\pi}{4} \frac{\sqrt{\alpha_0 \lambda_0}}{\beta_0} |H|^{-2/3} \ll 1. \quad (3.10)$$

This leads to  $D_1 \cong 1$  and  $D_2 \cong 1$ , and when these results are used in Eqs. (3.4) and (3.5), one arrives at the following explicit asymptotic expressions for  $\alpha_0$ ,  $\beta_0$ ,  $\lambda_0$ :

$$\beta_0 = \frac{1}{p_1 + p_2 \frac{H_1 \rho_1}{H_2 \rho_2}}, \quad (3.11)$$

$$\lambda_0 = p_1 \nu_1 + \frac{\rho_2}{\rho_1} p_2 \nu_2, \quad (3.12)$$

$$\alpha_0 = \frac{\left(\frac{\pi}{4} p_1 p_2\right)^{2/3} \left|1 - \frac{H_1 \rho_1}{H_2 \rho_2}\right|^{4/3} \left(p_1 \nu_1 + \frac{\rho_2}{\rho_1} p_2 \nu_2\right)^{1/3}}{\left(p_1 + p_2 \frac{H_1 \rho_1}{H_2 \rho_2}\right)^2}. \quad (3.13)$$

Note that  $\alpha_0 = 0$  when the Hall resistivities of the two constituents are equal  $H_1 \rho_1 = H_2 \rho_2$ . Moreover, when  $\rho_2/\rho_1 \gg 1$ , then  $\beta_0$  tends to the finite value  $1/p_1$ , while  $\lambda_0$  and  $\alpha_0$  both diverge. As we shall see in Section IV C 2 below, this behavior presages the behavior exhibited by those parameters when the No. 2 constituent is a perfect insulator, i.e., when  $\rho_2 = \infty$ .

A similar asymptotic dependence of the transverse relative bulk effective magnetoresistance on magnetic field was found previously for a free-electron-metal host with open orbit inclusions.<sup>15</sup> A similar asymptotic dependence was also previously found by Dreizin and Dykhne, who presented a qualitative microscopic discussion of magnetotransport in composite media.<sup>19</sup> In our language, those results would translate into  $\alpha \propto |H|^{2/3}$ , as we have also found. While the asymptotic behavior found in those previous studies is similar to what we find here, the present discussion shows that (a) one does not need to have open orbits in any constituent in order to observe this kind of behavior, (b) the behavior we find is a straightforward consequence of SEMA. Since SEMA becomes exact in the dilute limit, when either  $p_1$  or  $p_2$  is very small, we believe that the asymptotic result  $\alpha \propto |H|^{2/3}$  is exact. It appears that the only requirement for obtaining this type of asymptotic response is that the two constituents have comparable Ohmic resistivities and different Hall resistivities. In fact, our numerical solutions of these equations also suggest that only the difference in the Hall resistivities is crucial: The  $|H|^{2/3}$  power law is obtained even if the two constituents have *the same Ohmic resistivities*.

In order to confirm that our ansatz for the asymptotic behavior is indeed correct, we have solved the SEMA equations numerically for a simple example. We assume that  $\rho_1 = \rho_2$ ,  $\nu_1 = \nu_2 = 1$ , and  $H \equiv H_1 = 2H_2$ , and we consider  $p_1 = p_2 = 0.5$ . In Fig. 1(a) we plot the relative bulk effective transverse magnetoresistivity  $\alpha - 1$  vs.  $|H|^{2/3}$ . It is evident that this quantity rapidly approaches a linear dependence on  $|H|^{2/3}$  as  $|H|$  increases, and that the asymptotic dependence found analytically above is accurately achieved for  $|H| > 2$  for this choice of parameters. In Fig. 1(b), we plot the quotient  $\beta/H = \rho_{\text{Hall}}^{(e)}/\rho_{\text{Hall}}^{(1)}$  vs.  $|H|^{2/3}$ . The second form of this quotient shows that it is equal to the ratio of bulk effective Hall resistivity to the Hall resistivity of the No. 1 constituent, suggesting the name “relative Hall resistivity”. Clearly,  $\beta$  also rapidly approaches its asymptotic dependence upon  $H$ , which is linear rather than  $\propto |H|^{2/3}$  i.e., the ratio  $\beta/H$  becomes field-independent.

## IV. THREE-CONSTITUENT $M/I/S$ MIXTURES

### A. General considerations

Next, we turn to a discussion of a three-constituent composite containing a volume fraction  $p_M$  of normal metal,  $p_S$  of perfect conductor, and  $p_I$  of insulator. As part of this discussion, we will consider the special cases of two-constituent  $N/S$  and  $N/I$  mixtures. We use the subscripts  $M$ ,  $I$ , and  $S$  to denote normal metal, insulator, and perfect conductor.

We assume the following forms and inequalities for the bulk effective resistivity tensor  $\hat{\rho}_e$ , and for the three constituent resistivity tensors  $\hat{\rho}_M$ ,  $\hat{\rho}_I$ ,  $\hat{\rho}_S$ :

$$\hat{\rho}_e = \rho_M \begin{pmatrix} \alpha & -\beta & 0 \\ \beta & \alpha & 0 \\ 0 & 0 & \lambda \end{pmatrix}, \quad \hat{\rho}_M = \rho_M \begin{pmatrix} 1 & -H & 0 \\ H & 1 & 0 \\ 0 & 0 & \nu \end{pmatrix}, \quad (4.1)$$

$$\hat{\rho}_S = \rho_S \hat{I}, \quad \hat{\rho}_I = \rho_I \hat{I}, \quad \rho_S \ll \rho_M \ll |H| \rho_M \ll \rho_I, \quad (4.2)$$

where  $\hat{I}$  is the unit tensor. We use the results of Eqs. (2.7) and (2.8) in Eq. (2.5) for this system, and then take the limits  $\rho_S \rightarrow 0$  and  $\rho_I \rightarrow \infty$  to get the following equations for  $\alpha$ ,  $\beta$ ,  $\lambda$  from the  $zz$ ,  $xy$ , and  $xx$  components of that equation [again, the other components of Eq. (2.5) lead either to redundancies or to identities;  $p_M$ ,  $p_I$ ,  $p_S$  denote the constituent volume fractions, which satisfy  $p_M + p_I + p_S = 1$ ]

$$\frac{\lambda}{\nu} = \frac{1 - n_z}{n_z} \frac{n_z - p_S}{p_S + p_M - n_z}, \quad (4.3)$$

$$\frac{\beta}{\alpha^2 + \beta^2} = p_M \frac{H}{1 + H^2} \left/ \left( \frac{D_M}{D_I} p_I + p_M \right) \right., \quad (4.4)$$

$$\begin{aligned} & \left( \frac{D_M}{D_I} p_I + p_M \right) \left( \frac{\alpha}{\alpha^2 + \beta^2} - \frac{n_x}{\alpha} \right) - D_M \frac{p_S}{n_x} \frac{\alpha}{\alpha^2 + \beta^2} = \\ & = \frac{p_M}{1 + H^2} \left[ 1 + n_x \left( \frac{\alpha^2 + \beta^2}{\alpha} - 2 - \frac{2\beta H}{\alpha} \right) \right], \end{aligned} \quad (4.5)$$

where

$$\begin{aligned} D_M &= \left( 1 - n_x + n_x \frac{\alpha^2 + \beta^2}{\alpha(1 + H^2)} \right)^2 \\ &+ \frac{n_x^2 \beta^2}{\alpha^2} \left( 1 - \frac{\alpha^2 + \beta^2}{\beta} \frac{H}{1 + H^2} \right)^2, \end{aligned} \quad (4.6)$$

$$D_I = (1 - n_x)^2 + \frac{n_x^2 \beta^2}{\alpha^2}. \quad (4.7)$$

Combining Eqs. (4.4) and (4.5) we can simplify Eq. (4.5) slightly to get

$$\begin{aligned} & 1 + n_x \left[ \frac{\alpha^2 + \beta^2}{\alpha} \left( 1 + \frac{H}{\beta} \right) - 2 - \frac{2\beta H}{\alpha} \right] = \\ & = \frac{\alpha H}{\beta} - D_M \frac{p_S}{p_M} \frac{1 + H^2}{n_x} \frac{\alpha}{\alpha^2 + \beta^2}. \end{aligned} \quad (4.8)$$

Despite the seemingly simple form of Eqs. (4.3) and (4.4), the right hand sides of those equations do not constitute explicit expressions for  $\lambda$  or for  $\beta/(\alpha^2 + \beta^2)$ , because those right hand sides depend upon  $\alpha$ ,  $\beta$ ,  $\lambda$  through  $n_z$  and  $n_x$ . Nevertheless, Eq. (4.3) does show that  $n_z$  must satisfy the following inequalities in order for  $\lambda$  to be positive:

$$p_S < n_z < p_S + p_M = 1 - p_I, \quad (4.9)$$

where the lower bound must satisfy  $p_S < p_c = 1/3$  and the upper bound must satisfy  $p_S + p_M > p_c = 1/3$  (as before,  $p_c$  denotes the percolation threshold, equal to  $1/3$  in SEMA) in order for the entire composite to have a finite, nonzero bulk effective conductivity.

Eqs. (4.3)–(4.8) do not admit closed form solutions. In order to obtain asymptotic solutions when  $|H| \gg 1$ , we tried a range of possible ansatzes for the asymptotic forms of  $\alpha$ ,  $\beta$ ,  $\lambda$ , and proceeded to examine them for mathematical consistency and physical admissibility. Only three of those ansatzes stand up to both requirements; each is valid for a different range of the constituent volume fractions  $p_M$ ,  $p_I$ ,  $p_S$ , where, of course,  $p_M + p_I + p_S = 1$ . The three ansatzes and the resulting solutions are described in the following subsections.

## B. The saturating regime

### 1. General case

The first ansatz that leads to admissible results is

$$\alpha \cong \alpha_0, \quad \lambda \cong \lambda_0, \quad \beta \cong \frac{\beta_0}{H}. \quad (4.10)$$

This leads to the following results:

$$D_M \cong (1 - n_x)^2, \quad D_I \cong (1 - n_x)^2 \Rightarrow \frac{D_M}{D_I} \cong 1. \quad (4.11)$$

Consequently, Eq. (4.4) yields the following relation between  $\beta_0$  and  $\alpha_0$

$$\beta_0 = \alpha_0^2 \frac{p_M}{p_I + p_M}. \quad (4.12)$$

Using this to eliminate  $\beta_0$  from Eq. (4.8), we get

$$\begin{aligned} 0 &\cong \frac{1 - n_x}{\alpha_0 n_x p_M} (p_S - n_x) \Rightarrow n_x \cong p_S < \frac{1}{3} \Rightarrow \\ \Rightarrow n_z &= 1 - 2n_x \cong 1 - 2p_S = p_M + p_I - p_S > \frac{1}{3}. \end{aligned} \quad (4.13)$$

A consequence of the last inequality for  $n_z$  is that the transformed shape of the spherical inclusions is an *oblate spheroid*. Since we must also have [see Eq. (4.9)]

$$1 - 2p_S \cong n_z < p_S + p_M = 1 - p_I, \quad (4.14)$$

we find that we need to require  $2p_S > p_I$  in order for this asymptotic solution to be valid. Eq. (4.3) now becomes

$$\lambda_0 = \nu \frac{2p_S(1 - 3p_S)}{(1 - 2p_S)(2p_S - p_I)}. \quad (4.15)$$

In order to determine  $\alpha_0$  we first need to solve the following transcendental equation for the eccentricity  $e$  of the oblate spheroid:

$$n_z = \frac{1 + e^2}{e^3} (e - \arctan e) \cong 1 - 2p_S > \frac{1}{3}, \quad (4.16)$$

and then use the relation between  $e$  and  $\alpha$ ,  $\beta$ ,  $\lambda$

$$\begin{aligned} e &= \left( \frac{\alpha^2 + \beta^2}{\alpha\lambda} - 1 \right)^{1/2} \cong \left( \frac{\alpha_0}{\lambda_0} - 1 \right)^{1/2} \equiv e_0 \Rightarrow \\ \Rightarrow \alpha_0 &= \lambda_0(1 + e_0^2). \end{aligned} \quad (4.17)$$

These asymptotic results are valid for the range of constituent compositions defined by

$$\frac{p_I}{2} < p_S < \frac{1}{3}. \quad (4.18)$$

When  $p_S \rightarrow p_I/2$  from above,  $\alpha_0$ ,  $\lambda_0$ , and  $\beta_0$  all diverge, but at different rates:

$$\alpha_0 \propto \frac{1}{2p_S - p_I}, \quad \lambda_0 = \frac{\alpha_0}{1 + e_0^2} \propto \frac{1}{2p_S - p_I}, \quad (4.19)$$

$$\beta_0 \propto \frac{1}{(2p_S - p_I)^2}. \quad (4.20)$$

It is worth noting that  $\alpha$  and  $\lambda$  are both proportional to  $\nu$ . Along with the fact that they are asymptotically independent of  $H$ , this indicates that the local electric field in the  $M$  constituent is directed mostly along  $\mathbf{B}$ . Similar proportionality is also found in the two-constituent  $M/S$  case, discussed below. It is also worth noting that when  $p_S \rightarrow 1/3$  from below, then also  $n_z \rightarrow 1/3$ , and consequently  $e_0 \rightarrow 0$ . Both  $\alpha_0$  and  $\lambda_0$  tend to 0 as  $1 - 3p_S$ , but  $\alpha_0/\lambda_0 \rightarrow 1$ . This indicates that when the  $S$  constituent approaches its percolation threshold  $p_c = 1/3$ , the *same current flow paths* in the  $M$  constituent are responsible for the leading contribution to the macroscopic response *whatever the direction of the average current density*  $\langle \mathbf{J} \rangle$ .

## 2. Two-constituent $M/S$ mixture

An important special case of a three-constituent composite with saturating behavior is  $p_I = 0$ , corresponding to a two-constituent  $M/S$  mixture. One can also get the results for this case by setting  $p_I = 0$  in Eqs. (4.3), (4.4) [or alternatively by taking the limit  $\rho_1/\rho_2 \rightarrow \infty$  in Eqs. (3.3), (3.4)] to obtain the following equations:

$$\lambda = \nu \left( 1 - \frac{p_S}{n_z} \right), \quad \frac{\beta}{\alpha^2 + \beta^2} = \frac{H}{1 + H^2}, \quad (4.21)$$

and noting that Eq. (4.5) [or Eq. (3.5)] is satisfied as an identity to leading order in  $1/H$ .

The asymptotic large  $|H|$  behavior can then be obtained by using the ansatz of Eqs. (4.10). The second of Eqs. (4.21) immediately leads to a simple relation between  $\beta_0$  and  $\alpha_0$ , namely

$$\beta_0 = \alpha_0^2. \quad (4.22)$$

The value of the ratio  $\alpha_0/\lambda_0$  is obtained by first solving the transcendental equation for the asymptotic eccentricity  $e_0$ , namely

$$n_z \cong p_M - p_S = \frac{1 + e_0^2}{e_0^3} (e_0 - \arctan e_0), \quad (4.23)$$

and then using

$$e_0 \cong \left( \frac{\alpha_0}{\lambda_0} - 1 \right)^{1/2}. \quad (4.24)$$

Finally, the first of Eqs. (4.21) leads to

$$\lambda_0 \cong \nu \left( 1 - \frac{p_S}{p_M - p_S} \right) = \nu \frac{1 - 3p_S}{p_M - p_S}. \quad (4.25)$$

The fact that  $\alpha_0, \beta_0, \lambda_0$  all depend upon  $\nu$ , i.e.,  $\alpha_0 \propto \nu$ ,  $\lambda_0 \propto \nu$ ,  $\beta_0 \propto \nu^2$ , indicates that the leading contribution to the macroscopic response is due to local currents that flow parallel to  $\mathbf{B}$  in the  $M$  constituent.

When  $p_S$  approaches the SEMA percolation threshold value  $1/3$  from below, then  $n_z \rightarrow 1/3$ ; hence  $e_0 \rightarrow 0$  and  $\alpha_0/\lambda_0 \rightarrow 1$  from above. Both  $\alpha_0$  and  $\lambda_0$  tend to 0 as  $1 - 3p_S$ , while  $\beta_0 \rightarrow 0$  as  $(1 - 3p_S)^2$ . The fact that  $\lambda_0/\alpha_0 \rightarrow 1$  again indicates that the *same current flow paths* in the  $M$  constituent are responsible for the leading contribution to the macroscopic response *whatever the direction of the average current density*  $\langle \mathbf{J} \rangle$ .

The SEMA equations for an  $M/S$  mixture were treated numerically in the past.<sup>14</sup> Those calculations are in agreement with the asymptotic  $p_M$  dependence of  $\alpha_0, \lambda_0$ , and  $\beta_0$  obtained for such mixtures in this subsection.

## C. The non-saturating regime

### 1. General case

Another ansatz which leads to an admissible solution is

$$\alpha \cong \alpha_0 |H|, \quad \lambda \cong \lambda_0 |H|, \quad \beta \cong \beta_0 H. \quad (4.26)$$

Because  $\lambda$  is now very large, Eq. (4.3) leads to the following results

$$n_z \cong p_S + p_M - \mathcal{O} \left( \frac{1}{|H|} \right) = 1 - p_I - \mathcal{O} \left( \frac{1}{|H|} \right), \quad (4.27)$$

$$n_x = \frac{1}{2}(1 - n_z) \cong \frac{p_I}{2} + \mathcal{O} \left( \frac{1}{|H|} \right). \quad (4.28)$$

Since  $p_I < 2/3$ , we must have  $n_z > 1/3$  if  $|H|$  is large enough, and the transformed spherical inclusion is then again an oblate spheroid.

Instead of using the unknowns  $\alpha_0, \beta_0$ , it is convenient to introduce the variables  $x$  and  $y$ , defined by



$$x \equiv \frac{\alpha_0^2 + \beta_0^2}{\beta_0} > 1, \quad y \equiv \frac{\beta_0}{\alpha_0}. \quad (4.29)$$

Using  $x$  and  $y$ , we can write

$$D_M \cong \left(1 - \frac{p_I}{2}\right)^2 + \frac{p_I^2 y^2}{4} (1 - x)^2, \quad (4.30)$$

$$D_I \cong \left(1 - \frac{p_I}{2}\right)^2 + \frac{p_I^2 y^2}{4}. \quad (4.31)$$

Eq. (4.4) now becomes

$$(xp_M - p_M - p_I)[(2 - p_I)^2 + p_I^2 y^2] \cong p_I^3 y^2 (x^2 - 2x), \quad (4.32)$$

while Eq. (4.8) becomes

$$\begin{aligned} p_I x (xy^2 + 1 + y^2) &\cong \\ &\cong 2p_I xy^2 + 2x - \frac{p_S}{p_M p_I} [(2 - p_I)^2 + p_I^2 y^2 (1 - x)^2]. \end{aligned} \quad (4.33)$$

These equations are both linear in  $y^2$ . When  $y^2$  is eliminated, the result is a factorizable cubic equation for  $x$

$$\begin{aligned} 0 &= x[x^2(2 - 3p_I) - x(4 + 2p_S - 5p_I) + 2(1 + p_S - p_I)] \\ &= x(x - 1) \left[ x - 2 \left( \frac{1 + p_S - p_I}{2 - 3p_I} \right) \right] (2 - 3p_I). \end{aligned} \quad (4.34)$$

Since  $p_I = 1 - p_S - p_M < 2/3$ , the physical solution is obviously

$$x = 2 \frac{1 + p_S - p_I}{2 - 3p_I} = \frac{2(2p_S + p_M)}{2 - 3p_I} > 0. \quad (4.35)$$

This leads to an expression for  $y^2$  which is a quotient of somewhat complicated polynomials in  $p_M, p_I, p_S$ . Those can be factorized, after some effort, leading to

$$y^2 = \frac{(2 - 3p_I)(2 - p_I)(p_I - 2p_S)}{p_I^2(2p_S + p_I)}, \quad (4.36)$$

which is positive if  $p_I > 2p_S$ . These results lead to the following expressions for  $\alpha_0, \beta_0$

$$\beta_0 = \frac{(2p_S + p_M)(1 + p_M + p_S)(p_I/2 - p_S)}{p_I(1 - p_I)^2 + p_S[2 - (2 - p_I)^2]}, \quad (4.37)$$

$$\begin{aligned} \alpha_0 &= \left( \frac{(p_I - 2p_S)(2p_S + p_I)(1 + p_M + p_S)}{2 - 3p_I} \right)^{1/2} \\ &\quad \times \frac{p_I(p_S + p_M/2)}{p_I(1 - p_I)^2 + p_S[2 - (2 - p_I)^2]}. \end{aligned} \quad (4.38)$$

Obviously, the cubic polynomial which appears in the denominators of  $\alpha_0, \beta_0$  is positive over the entire range  $0 < 2p_S < p_I$  where Eqs. (4.37) and (4.38) are applicable. Finally,  $\lambda_0$  can again be found by first solving the following transcendental equation for the eccentricity  $e$  of the oblate spheroid

$$n_z = \frac{1 + e^2}{e^3} (e - \arctan e) \cong p_S + p_M, \quad (4.39)$$

and then using the relation between  $e$  and  $\alpha, \beta, \lambda$  to get

$$e = \left( \frac{\alpha^2 + \beta^2}{\alpha\lambda} - 1 \right)^{1/2} \cong \left( \frac{\alpha_0^2 + \beta_0^2}{\alpha_0\lambda_0} - 1 \right)^{1/2}. \quad (4.40)$$

These asymptotic results are valid for the range of constituent compositions defined by

$$p_S < \frac{p_I}{2} < \frac{1}{3}. \quad (4.41)$$

When  $p_S$  approaches  $p_I/2$  from below, then  $\alpha_0$ ,  $\beta_0$ ,  $\lambda_0$  all tend to 0, but at different rates:

$$\alpha_0 \propto \sqrt{p_I - 2p_S}, \quad \lambda_0 \cong \frac{\alpha_0}{1 + e^2} \propto \sqrt{p_I - 2p_S}, \quad (4.42)$$

$$\beta_0 \propto p_I - 2p_S. \quad (4.43)$$

It is worth noting that  $\alpha$ ,  $\beta$ , and  $\lambda$  are all independent of  $\nu$ . This indicates that the local electric field in the  $M$  constituent has considerable components that are perpendicular to  $\mathbf{B}$ . It is also worth noting that, when  $p_I \rightarrow 2/3$ , both  $\alpha_0$  and  $\lambda_0$  diverge but  $\alpha_0/\lambda_0 \rightarrow 1$ , i.e.,

$$\alpha_0 \cong \lambda_0 \cong 2 \left( \frac{1 - 9p_S^2}{3(2 - 3p_I)} \right)^{1/2}. \quad (4.44)$$

This indicates that, when the total volume fraction of conducting constituents  $p_M + p_S$  approaches its percolation threshold  $p_c = 1/3$ , the *same current flow paths* in the  $M$  constituent are responsible for the leading contribution to the macroscopic response *whatever the direction of the average current density*  $\langle \mathbf{J} \rangle$ .

## 2. Two-constituent $M/I$ mixture

An important special case within the nonsaturating regime is  $p_S = 0$ , corresponding to a two-constituent  $M/I$  mixture. One can also get the results for such a mixture by setting  $p_S = 0$  in Eqs. (4.3), (4.4), and (4.8) to get the following equations:

$$\lambda = \nu \frac{1 - n_z}{p_M - n_z}, \quad (4.45)$$

$$\frac{\beta}{\alpha^2 + \beta^2} \left( \frac{p_I}{p_M} \frac{D_M}{D_I} + 1 \right) = \frac{H}{1 + H^2}, \quad (4.46)$$

$$\frac{\alpha}{n_x} \left( \alpha - \frac{\beta}{H} \right) = (\alpha^2 + \beta^2) \left( 1 + \frac{\beta}{H} \right) - 2\beta \left( \beta + \frac{\alpha}{H} \right). \quad (4.47)$$

The asymptotic behavior is obtained by making the ansatz of Eqs. (4.26). After a sequence of algebraic steps similar to those described above, the following results are obtained for the asymptotic linear slopes:

$$\beta_0 = \frac{1 + p_M}{2p_M}, \quad \alpha_0 = \frac{p_I}{2p_M} \left( \frac{1 + p_M}{3p_M - 1} \right)^{1/2}, \quad (4.48)$$

$$\lambda_0 = \alpha_0 \frac{(2p_M/p_I)^2}{1 + e_0^2}, \quad (4.49)$$

where  $e_0$  is given implicitly in terms of  $p_M$  by the transcendental equation

$$p_M = \frac{1 + e_0^2}{e_0^3} (e_0 - \arctan e_0), \quad (4.50)$$

which must be solved numerically. As in the  $M/I/S$  nonsaturating regime,  $\alpha_0$ ,  $\beta_0$ ,  $\lambda_0$  are all independent of  $\nu$ . This indicates that the leading contribution to the macroscopic or bulk effective response is due to local currents that flow perpendicular to  $\mathbf{B}$  in the  $M$  constituent.

When  $p_M$  approaches the SEMA percolation threshold value of  $1/3$  from above, then  $\beta_0 \rightarrow 2$  and  $e_0 \rightarrow 0$ . Therefore  $\lambda_0/\alpha_0 \rightarrow 1$  from above, and both  $\alpha_0$  and  $\lambda_0$  diverge as  $1/\sqrt{3p_M - 1}$ . The fact that  $\lambda_0/\alpha_0 \rightarrow 1$  again indicates that the *same current flow paths* in the  $M$  constituent are responsible for the leading contribution to the macroscopic response *whatever the direction of the average current density*  $\langle \mathbf{J} \rangle$ .

Once again, in order to confirm the asymptotic behavior predicted analytically, we have solved the SEMA equations numerically. We assume  $\nu_1 \equiv \nu = 1$  [see Eq. (3.1)],  $\hat{\rho}_2 = \infty$ , and consider a variety of values of  $p_1 \equiv p_M$  above the

percolation threshold  $p_c$  (equal to  $1/3$  in the SEMA in three dimensions). The resulting behavior of  $\alpha$  and  $\lambda$  is shown in Figs. 2(a) and 2(b); we also show the relative Hall resistivity  $\beta/H$  in Fig. 2(c). Evidently, for any choice of  $p_M$ ,  $\alpha$  and  $\lambda$  rapidly approach their asymptotic linear dependence on  $|H|$ , as predicted by the asymptotic analysis. Furthermore, the slope increases as  $p_M$  approaches the percolation threshold, again as predicted by the asymptotic results. The asymptotic linear dependence appears to be reached approximately when  $|H| > 5$ , for all the values of  $p_M$  that were considered. For  $p_M$  less than about  $0.5$ , we had some difficulty, using our simple algorithm, in solving the SEMA equations numerically; by contrast, of course, the asymptotic analysis gives the slope, for any value of  $p_M$  greater than  $p_c = 1/3$ , without any difficulty.

#### D. Scaling behavior near the transition point

If we compare the critical behaviors exhibited by  $\alpha$ ,  $\beta$ ,  $\lambda$  when  $|H| \gg 1$  and  $p_I \rightarrow 2p_S$  from above [Eqs. (4.42), (4.43)] and from below [Eqs. (4.19) and (4.20)], we are led to anticipate a scaling behavior. That is, we should be able to describe the critical behavior in both regimes by using a scaling variable which is some power of  $H^2(p_I - 2p_S)^3/\nu^2$ , and writing  $\alpha$ ,  $\beta$ ,  $\lambda$  in terms of three (scaling) functions of that variable. We have found that the most convenient scaling variable for this purpose is

$$Z \equiv \left( \frac{|H|}{\nu} \right)^{2/3} (p_I - 2p_S). \quad (4.51)$$

In the “critical region”, i.e., when  $|H| \gg 1$  and  $|p_I - 2p_S| \ll 1$ , the bulk effective resistivity parameters can now be expressed as

$$\alpha \cong \frac{\nu}{p_I - 2p_S} F_\alpha(Z), \quad (4.52)$$

$$\lambda \cong \frac{\nu}{p_I - 2p_S} F_\lambda(Z), \quad (4.53)$$

$$\beta \cong \frac{\nu^2}{H(p_I - 2p_S)^2} F_\beta(Z). \quad (4.54)$$

As usual, there are three important extreme regimes within the critical region, namely:  $Z < 0$ ,  $|Z| \gg 1$  (Regime I, where  $2p_S > p_I$ );  $Z > 0$ ,  $|Z| \gg 1$  (Regime II, where  $2p_S < p_I$ ); and  $|Z| \ll 1$  (Regime III, where we can have either  $2p_S > p_I$ , or  $2p_S < p_I$ , or  $2p_S = p_I$ ). The behavior of the scaling functions  $F_\alpha(Z)$ ,  $F_\lambda(Z)$ ,  $F_\beta(Z)$  in Regimes I and II is dictated by the critical behaviors found earlier. Their behavior in Regime III is dictated by the requirement that this behavior must exactly cancel the divergences that would otherwise occur due to the vanishing  $2p_S - p_I$  factor in the denominators of the above expressions. These considerations lead to the following forms for the scaling functions in the three regimes:

$$F_\alpha(Z) \cong \begin{cases} -A & \text{Regime I} \\ A'Z^{3/2} & \text{Regime II} \\ A''Z & \text{Regime III} \end{cases} \quad (4.55)$$

$$F_\lambda(Z) \cong \begin{cases} -L & \text{Regime I} \\ L'Z^{3/2} & \text{Regime II} \\ L''Z & \text{Regime III} \end{cases} \quad (4.56)$$

$$F_\beta(Z) \cong \begin{cases} B & \text{Regime I} \\ B'Z^3 & \text{Regime II} \\ B''Z^2 & \text{Regime III} \end{cases} \quad (4.57)$$

where the primed and double primed and unprimed versions of  $A$ ,  $B$ ,  $L$  are positive dimensionless constants of order 1. Their values can be found, if necessary, by comparing the resulting expressions for  $\alpha$ ,  $\beta$ ,  $\lambda$  with the detailed solutions of the SEMA equations. Qualitative plots of these scaling functions are shown in Fig. 3.

As indicated above, these equations make a nontrivial prediction about the behavior of  $\alpha$ ,  $\beta$ ,  $\lambda$  in Regime III, which was not worked out in the previous sections, namely:

$$\alpha \cong \alpha_0 |H|^{2/3}, \quad \lambda \cong \lambda_0 |H|^{2/3}, \quad \beta \cong \beta_0 |H|^{1/3} \text{sign}(H). \quad (4.58)$$

We now use these scaling forms as an ansatz for another asymptotic solution of the SEMA equations, assuming  $p_I = 2p_S$ , in order to check for consistency of the scaling scheme developed here.

Since  $\lambda$  is very large, Eq. (4.3) entails

$$n_z \cong p_S + p_M = 1 - p_I = 1 - 2p_S > \frac{1}{3}, \quad n_x \cong p_S < \frac{1}{3}, \quad (4.59)$$

where we have used the fact that  $p_I = 2p_S$ . From Eq. (4.3) we can also calculate the small correction to  $n_z \cong 1 - 2p_S$  in terms of  $\lambda_0$

$$1 - 2p_S - n_z \cong \frac{\nu}{\lambda_0 |H|^{2/3}} \frac{2p_S(1 - 3p_S)}{1 - 2p_S}. \quad (4.60)$$

In addition, we can write expressions for  $D_M$ ,  $D_I$ , and for their ratio  $D_M/D_I$ , that go *beyond* leading order in  $1/H$ , namely

$$D_M \cong (1 - n_x)^2 + \frac{n_x^2 \beta_0^2}{\alpha_0^2 |H|^{2/3}} \left(1 - \frac{\alpha_0^2}{\beta_0}\right)^2, \quad (4.61)$$

$$D_I \cong (1 - n_x)^2 + \frac{n_x^2 \beta_0^2}{\alpha_0^2 |H|^{2/3}}, \quad (4.62)$$

$$\frac{D_M}{D_I} \cong 1 + \frac{\alpha_0^2 - 2\beta_0}{|H|^{2/3}} \left(\frac{n_x}{1 - n_x}\right)^2. \quad (4.63)$$

From Eq. (4.4) we get a relation between  $\beta_0$  and  $\alpha_0$

$$\beta_0 = \alpha_0^2 \frac{1 - 3p_S}{1 - p_S}. \quad (4.64)$$

Using this result, we find that Eq. (4.5) becomes an identity to leading order in  $1/H$ . We therefore need to consider that equation in the next-to-leading order. The result is

$$1 - 2p_S - n_z \cong \frac{\alpha_0^2}{|H|^{2/3}} \frac{4p_S^2(1 - 3p_S)}{(1 - p_S)^3}. \quad (4.65)$$

Comparison of this equation with Eq. (4.60) yields the following relation between  $\alpha_0$  and  $\lambda_0$ :

$$\frac{\alpha_0^2 \lambda_0}{\nu} = \frac{(1 - p_S)^3}{2p_S(1 - 2p_S)}. \quad (4.66)$$

Another relation between those two unknowns is obtained by first solving the transcendental equation for the eccentricity  $e$  of the oblate spheroid

$$n_z = \frac{1 + e^2}{e^3} (e - \arctan e) \cong p_S + p_M, \quad (4.67)$$

and then using the expression for  $e$  in terms of  $\alpha$ ,  $\beta$ ,  $\lambda$  to get

$$1 + e^2 = \frac{\alpha^2 + \beta^2}{\alpha \lambda} \cong \frac{\alpha_0}{\lambda_0}. \quad (4.68)$$

Eqs. (4.64), (4.66), and (4.68) then provide a complete and consistent solution for  $\alpha_0$ ,  $\beta_0$ ,  $\lambda_0$ , obtained by jointly considering the scaling and SEMA equations.

Again, it is worth noting that both  $\alpha$  and  $\lambda$  are proportional to  $\nu^{1/3}$ , while  $\beta \propto \nu^{2/3}$ . This seems to be consistent with the fact that  $\alpha$  and  $\lambda$  are also proportional to  $|H|^{2/3}$ , while  $\beta \propto |H|^{4/3}/H$ . These behaviors indicate that the local current flows both parallel and perpendicular to  $\mathbf{B}$ , and that the three principal Ohmic conductivities of the  $M$  constituent all contribute to the macroscopic response when  $p_I = 2p_S$ .

## V. SUMMARY AND DISCUSSION

A striking result of the present work is that, in an  $M/I$  composite, both  $\rho_{\perp}^{(e)}$  and  $\rho_{\parallel}^{(e)}$  are proportional to  $|H|$  in the strong-field limit. Such *linear magnetoresistance* has long been a mysterious observed feature of transport in polycrystalline samples of even so-called “simple metals”.<sup>20</sup> This behavior has sometimes been ascribed to macroscopic inhomogeneities. But until now, only in the low-concentration limit has proof been given that such inhomogeneities could actually produce a linear magnetoresistance.<sup>11,21,12</sup> Here, we have shown that both  $\rho_{\perp}^{(e)}$  and  $\rho_{\parallel}^{(e)}$  remain linear in  $|H|$  even at *higher concentrations* of inclusions, provided those inclusions have *strictly zero conductivity*. This result may be relevant to a range of experimental systems.

It is quite easy to understand, qualitatively, the behavior of an  $M/S$  disordered mixture: Whatever the direction of the *average current density*  $\langle \mathbf{J} \rangle$ , the *local current density*  $\mathbf{J}(\mathbf{r})$  in the  $M$  constituent will flow mostly along  $\mathbf{B} \parallel z$  when  $H$  is very large, and this tendency will become more and more pronounced with increasing  $|H|$ . Components of  $\mathbf{J}(\mathbf{r})$  that are perpendicular to  $\mathbf{B}$  will have finite values only inside the  $S$  constituent, while in the  $M$  constituent they will tend to 0 as  $1/H^2$ . This results in a current flow pattern that saturates when  $|H| \gg 1$ ; therefore, all the Ohmic resistivities will also saturate. The Hall resistivity will be very small—of order  $1/H$ —because the local Hall field  $\mathbf{E}_H$  will also be of that order.

The behavior of  $M_1/M_2$  mixtures is more difficult to understand qualitatively. Our interpretation of the (successful) ansatz of Eq. (3.6) is that when  $\langle \mathbf{J} \rangle \parallel \mathbf{B} \parallel z$ , the current distribution saturates for large values of  $|H|$ . But when  $\langle \mathbf{J} \rangle \perp \mathbf{B}$ , then that distribution continues to evolve with increasing  $|H|$ , with the current distortions increasing asymptotically as  $|H|^{1/3}$ .

The macroscopic response of  $M/I$  mixtures is qualitatively similar to the behavior of an isolated insulating inclusion embedded in an  $M$  host, as shown many years ago by an exact solution for such an inclusion of spherical or cylindrical shape.<sup>21</sup> The fact that this kind of behavior persists down to the percolation threshold indicates that, despite the interactions between current distortions produced by different inclusions, the local current distribution never saturates as  $|H|$  increases. The results we got would require that the current distortions increase as  $|H|^{1/2}$  for large  $H$ . However, the fact that the coefficients  $\alpha_0$  and  $\lambda_0$  diverge as  $p_M \rightarrow p_c$  probably signals that those distortions increase even more rapidly than  $|H|^{1/2}$  precisely at the percolation threshold.

The present results can also be compared with some simulations performed previously on a discrete network model, where finite size  $L \times L \times L$  samples were considered precisely at the percolation threshold.<sup>22</sup> Those simulations showed that, when  $L$  is much less than a “magnetic correlation length”  $\xi_H \propto |H|^{0.46}$ , the Ohmic resistivities saturate at a value proportional to  $L^{6.7}$ . However, in the opposite limit  $L \gg \xi_H$ , the Ohmic resistivities continue to increase as  $|H|^{2.1} L^{2.2}$ . This result is consistent, within the error bars, with  $H^2 L^{t/\nu}$ , where  $t \cong 2.0$  and  $\nu \cong 0.89$  are the usual percolation critical exponents for scalar Ohmic conductivity ( $\sigma_e \propto \Delta p^t$ ,  $\Delta p \equiv p_M - p_c$ ) and for the percolation correlation length ( $\xi_p \propto \Delta p^{-\nu}$ )—see Ref. 23. Using finite size scaling to replace the system size  $L$  by  $\xi_p$  in these results, we are led to expect that

$$\alpha, \lambda \propto \begin{cases} \Delta p^{-4.0} & \text{for } \Delta p \gg |H|^{-0.52} \text{ or } \xi_p \ll \xi_H, \\ H^2 & \text{for } \Delta p \ll |H|^{-0.52} \text{ or } \xi_p \gg \xi_H. \end{cases} \quad (5.1)$$

Obviously, this behavior differs in a number of ways from what was found in Section IVC2 using SEMA. It is not surprising that the critical exponents predicted by SEMA are quantitatively incorrect. However, the fact that, according to the simulations, the magnetoresistivity saturates as  $|H| \rightarrow \infty$ , is qualitatively at odds with the predictions of SEMA. Clearly, this qualitative discrepancy needs to be examined further. We conjecture that it has to do with the existence of three diverging lengths in this problem, namely  $\xi_p$ ,  $\xi_H$ , and  $L$ .

The qualitative situations described above continue to be applicable also in the case of the three-constituent  $M/I/S$  mixtures. The presence or absence of system-spanning (i.e., infinite) current flow paths, which are parallel to  $\mathbf{B}$  inside the  $M$  constituent, now depends on the relative amounts of  $I$  and  $S$  inclusions. The critical points or transition points  $p_I = 2p_S$  can be expected to occur when such paths first appear with increasing  $p_S$ .

Obviously, this transition is a kind of percolation process. In fact, we believe it is a physical realization of “anisotropic percolation”. This kind of percolation was first considered many years ago in the context of a two-dimensional, randomly diluted, square bond network.<sup>24</sup> The geometrical properties of anisotropic percolation in hypercubic random bond networks of arbitrary dimension were also studied extensively.<sup>25,26</sup>

As originally defined, the anisotropic percolation problem is characterized by different occupation probabilities for bonds aligned along different principal axes of the network. This situation is not easily implemented in a continuum percolating system, because that would require an anisotropic constituent where the principal conductivities have ratios that are extremely different from 1. Also, the principal axes of different grains of that constituent would have to be *identically oriented*. While this may be difficult to achieve in conducting materials when  $\mathbf{B} = 0$ , such extreme

ratios and identical orientations can easily be attained, even in an isotropic conductor, just by applying a magnetic field such that  $|H| \gg 1$  or  $\nu \ll 1$ . In that case, if we identify volume fractions with the bond occupation probabilities, then we can say that, for  $|H| \gg 1$  or  $\nu \ll 1$ , the regions that are highly conducting along  $\mathbf{B}$  occupy a fraction  $p_M + p_S$  of the total volume. By contrast, the regions that are highly conducting perpendicular to  $\mathbf{B}$  occupy the smaller volume fraction  $p_S$ . Our SEMA result, for the transition points between saturating and non-saturating regimes of magnetoresistance, can then be interpreted as follows

$$\begin{aligned} 0 &= 1 - p_x - p_y - p_z = 1 - p_S - p_S - (p_M + p_S) \\ &= p_I - 2p_S, \end{aligned} \tag{5.2}$$

where  $p_z = p_M + p_S$  represents the bond occupation probability along  $\mathbf{B}$  while  $p_x = p_y = p_S$  represent the bond occupation probabilities in the directions perpendicular to  $\mathbf{B}$ .

The identification of the critical points in the  $M/I/S$  magnetoresistive response with an anisotropic percolation threshold needs to be verified by a more accurate treatment of the bulk effective magnetoresistance. In particular, it needs to be determined whether the ever-present Hall conductivity is an irrelevant perturbation, or whether it in fact destabilizes the usual percolation fixed point, or alters the critical behavior associated with it. In any case, we expect that such a treatment will yield different values for the critical exponents and different forms for the scaling functions and scaling variable than those obtained here using SEMA.

Experimental studies of the line of magnetoresistive critical points can be conducted on samples made by using a semiconductor host with a large Hall mobility  $\mu$  as the  $M$  constituent, in which two types of inclusions are randomly embedded: highly insulating inclusions (e.g., voids) as the  $I$  constituent, and either highly conducting normal metallic inclusions or superconducting inclusions as the  $S$  constituent.

## ACKNOWLEDGMENTS

We are grateful to Eivind Almaas for help with Figs. 1 and 2. This research was supported in part by grants from the US-Israel Binational Science Foundation, the Israel Science Foundation, and NSF Grant DMR 97-31511.

- 
- <sup>1</sup> D. A. G. Bruggeman, Ann. Physik (Leipzig) **24**, 636 (1935).
  - <sup>2</sup> R. Landauer, J. Appl. Phys. **23**, 779 (1952).
  - <sup>3</sup> B. Budiansky, J. Mech. Phys. Solids **13**, 223 (1965).
  - <sup>4</sup> R. Hill, J. Mech. Phys. Solids **13**, 213 (1965).
  - <sup>5</sup> D. J. Bergman, Phys. Rev. B **39**, 4598 (1989).
  - <sup>6</sup> D. J. Bergman, in *Composite Media and Homogenization Theory*, eds. G. Dal Maso and G. F. Dell'Antonio, Birkhäuser, Berlin, 1991, pp. 67–79.
  - <sup>7</sup> L. Sali and D. J. Bergman, J. Stat. Phys. **86**, 455 (1997).
  - <sup>8</sup> H. Stachowiak, Physica **45**, 481 (1970).
  - <sup>9</sup> D. Stroud, Phys. Rev. B **12**, 3368 (1975).
  - <sup>10</sup> M. H. Cohen and J. Jortner, Phys. Rev. Lett. **30**, 696 (1973).
  - <sup>11</sup> D. Stroud and F. P. Pan, Phys. Rev. B **13**, 1434 (1976).
  - <sup>12</sup> B. Ya. Balagurov, Fiz. Tverd. Tela **28**, 3012 (1986) [Sov. Phys. Solid State **28**, 1694 (1986)].
  - <sup>13</sup> D. Stroud and F. P. Pan, Phys. Rev. B **20**, 455 (1979).
  - <sup>14</sup> D. Stroud, Phys. Rev. Lett. **44**, 1708 (1980).
  - <sup>15</sup> F. P. Pan, PhD Thesis 1977, The Ohio State University, unpublished.
  - <sup>16</sup> D. J. Bergman and Y. M. Strelniker, Phys. Rev. B **60**, 13016 (1999).
  - <sup>17</sup> D. J. Bergman, rejected by PRL.
  - <sup>18</sup> L. D. Landau, E. M. Lifshitz, and L. P. Pitaevskii, *Electrodynamics of Continuous Media*, 2nd edition, Pergamon Press, New York, 1984.
  - <sup>19</sup> Yu. A. Dreizin and A. M. Dykhne, Zh. Eksp. Teor. Fiz. **63**, 242 (1972) [Sov. Phys.–JETP **36**, 127 (1973)].
  - <sup>20</sup> P. Kapitza, Proc. Roy. Soc. **A123**, 292 (1929).
  - <sup>21</sup> J. B. Sampsell and J. C. Garland, Phys. Rev. B **13**, 583 (1976).
  - <sup>22</sup> A. K. Sarychev, D. J. Bergman, and Y. M. Strelniker, Phys. Rev. B **48**, 3145 (1993).
  - <sup>23</sup> A. Aharony and D. Stauffer, *Introduction to Percolation Theory*, 2nd edition, Taylor and Francis, London, 1992.
  - <sup>24</sup> M. F. Sykes and J. W. Essam, Phys. Rev. Lett. **10**, 3 (1963).
  - <sup>25</sup> S. Redner and H. E. Stanley, J. Phys. A: Math. Gen. **12**, 1267 (1979).

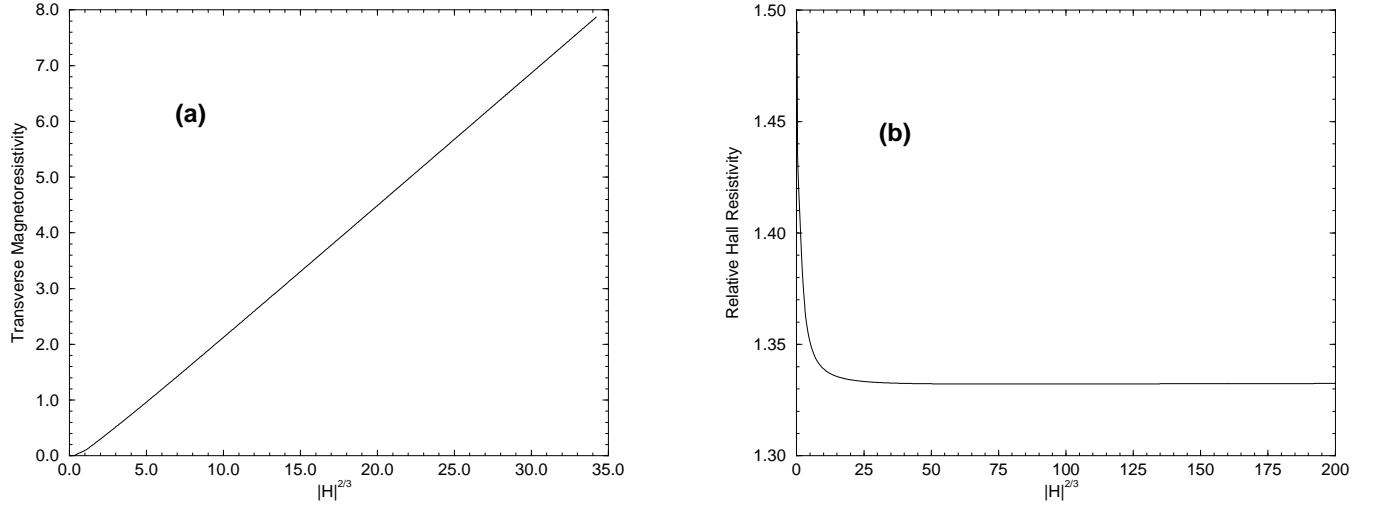
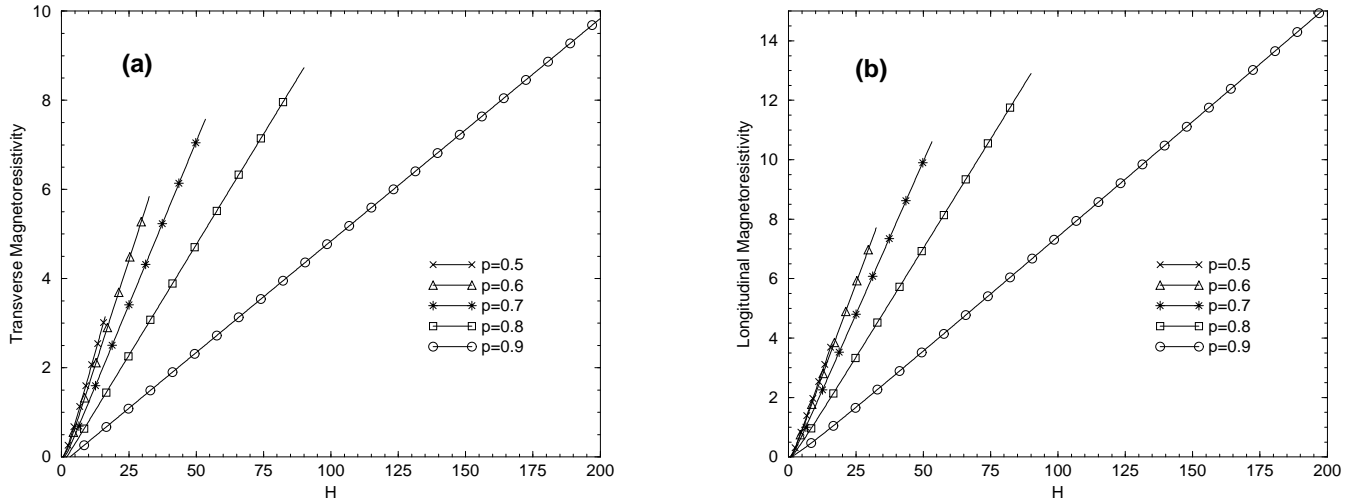


FIG. 1. Results of numerical solution of the SEMA Eqs. (3.3)–(3.5) for an  $M_1/M_2$  mixture. (a) Plot of the relative bulk effective transverse magnetoresistivity  $\alpha - 1$  vs.  $|H|^{2/3}$  for a three-dimensional composite of two free-electron-metal constituents, present in equal amounts  $p_1 = p_2 = 1/2$ , which have the same ohmic resistivity, but Hall resistivities that differ by a factor two [i.e.,  $\rho_1 = \rho_2$  and  $H_1 = H$ ,  $H_2 = 2H$ , in the notation of Eq. (3.1)]. (b) Same as (a), except that we plot the relative bulk effective Hall resistivity  $\beta(H)/H$  vs.  $|H|^{2/3}$  [cf. Eq. (3.2)].



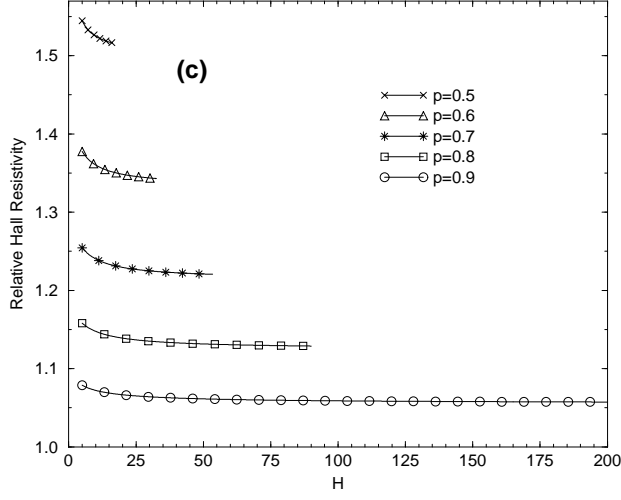


FIG. 2. Results of numerical solution of the SEMA Eqs. (4.45)–(4.47) for an  $M/I$  mixture. (a) Plot of the relative bulk effective transverse magnetoresistivity  $\alpha - 1$  vs.  $|H|$  for a three-dimensional two-constituent composite of free-electron metal and perfect insulator for various values of the metal volume fraction  $p \equiv p_M$ . (b) Same as (a), except that we plot the relative bulk effective longitudinal magnetoresistivity  $\lambda - 1$ . (c) Same as (a), except that we plot the relative bulk effective Hall resistivity  $\beta(H)/H$  vs.  $|H|$  only at high fields ( $|H| > 5$ ).

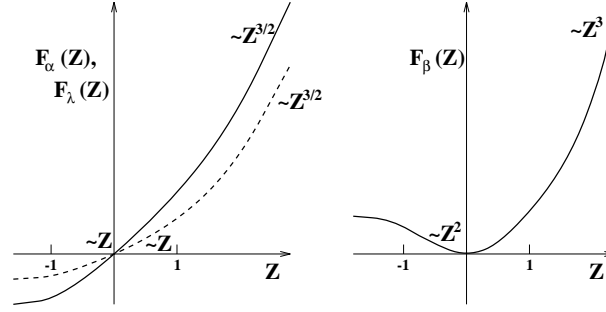


FIG. 3. Qualitative plots of the scaling functions obtained using SEMA. The left plot shows  $F_\alpha(Z)$  (solid line) and  $F_\lambda(Z)$  (dashed line), which are similar but not identical, with  $|F_\alpha(Z)| > |F_\lambda(Z)|$ , while the right plot shows  $F_\beta(Z)$ , which is never negative.